2006

Numerical Simulation on Scroll Expander-Compressor Unit for CO2 Trans-Critical Cycles

Hyunjin Kim
University of Incheon

Jongmin Ahn
University of Incheon

Sungouk Cho
Samsung Electronics Co.

Kyungrae Cho
Samsung Electronics Co.

NUMERICAL SIMULATION ON SCROLL EXPANDER-COMPRESSOR UNIT FOR CO_2 TRANS-CRITICAL CYCLES

Hyun Jin Kim[1]*, Jong Min Ahn[2] ,Sung Ouk Cho[3], Kyung Rae Cho[4]

[1,2]Department of Mechanical Engineering, University of Incheon
177 Dohwa-dong, Nam-gu, Incheon, Korea
[1]E-mail : kimhj@incheon.ac.kr
[3,4] DA R&D Center, Digital Appliance Business, Samsung Electronics Co., Ltd, Suwon, Korea
[3]E-mail : so.cho@samsung.com, [4]E-mail : kr0007.cho@samsung.com

ABSTRACT

In a two-stage compression CO_2 trans-critical cycle, application of a combined scroll expander-compressor unit has been considered in order to improve the cycle COP. For the combined scroll expander-compressor unit, power was recovered from a scroll expander which replaced the expansion valve and transmitted to the first stage auxiliary compressor which was directly coupled to the expander through a common crankshaft. Numerical simulation on its performance showed that for the suction pressure of 3.5MPa, discharge pressure of 10MPa with expander inlet temperature of 35^{o}C, the main compressor input could be reduced by 12.1% by the expander output. Increase in the cooling capacity by the expander was 8.6%. As a consequence, COP improvement of the cycle was estimated to be 23.5% by the application of this expander-compressor unit. COP improvement increased with lowering the expander inlet temperature, but decreased with increasing the suction pressure. Performance of the scroll expander was relatively insensitive to changes of operating pressure ratio, whereas that of the scroll compressor decreased rapidly as the operating pressure ratio became far from the design pressure ratio.

1. INTRODUCTION

Since CO_2 has favorable environmental properties and it is inflammable and nontoxic, it is regarded as one of the most promising natural fluids for substituting for HCFCs and HFCs. One of the major drawbacks in using CO2 for air-conditioning or heat pump applications is the low system efficiency. It has been reported, however, that if the throttling loss associated with expansion process can be recovered in CO_2 cycles, the CO_2 systems could become competitive with systems using other refrigerants. One way of doing this is to make the expansion process isentropic rather than isenthalpic. Some have proposed using expander for such purpose(Nickl *et al*, 2003; Zha *et al*, 2003; Fukuta *et al*, 2003; Preissner, 2001 ; Westphalen and Dieckmann, 2004).

Basically, since an expander can be understood as a compressor run in reverse, various types of compression mechanisms have been considered to be adopted for CO_2 expander: reciprocating, rolling piston rotary, vane rotary, and scroll types. Nickl *et al*(2003) developed a series of reciprocating expander-compressor units. About 30% of COP improvement was reported in an experimental CO_2 refrigeration loop equipped with their first generation expander-compressor when it was in the so-called full-pressure mode. Rolling piston type expander was studied by Zha *et al*(2003). For the reciprocating and rolling piston types, however, control of valve openings was needed to ensure proper operation. Vane rotary type expander was considered by Fukuta *et al*(2003). They set up a mathematical model to examine the performance of a vane rotary expander. Total expander efficiency was calculated to be around 40% at about 2000rpm, bringing in 20% COP improvement. Testing of expander prototype at slightly smaller pressure ratio showed total expander efficiency of 43%.

Preissner(2001) carried out theoretical analysis on the effects of scroll type expander use in air conditioning systems on the system performance: About 40-65% COP improvement could be obtained in CO_2 system, but only one third of that improvement was found in R134a system. In testing of scroll expander prototype, internal leakage in expansion chambers was found critical to the scroll expander performance. Westphalen and Dieckmann(2004) performed scroll expander design for 10.5kW CO_2 air conditioning system. They estimated that about 20% of the compressor input for the CO_2 system could be reduced by using the designed expander.

In this study, a combined scroll expander-compressor unit has been designed as a means of recovering the throttling loss in a two-stage compression trans-critical CO_2 cycle and its performance has been analytically investigated over ranges of operating pressures and the expander inlet temperature.

2. SCROLL EXPANDER-COMPRESSOR UNIT

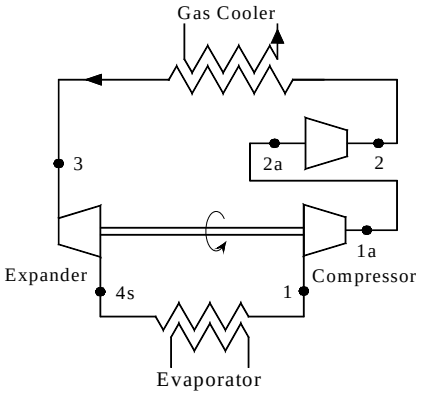

Fig. 1 Schematic diagram of a CO_2 heat pump water heater cycle with expander-compressor unit

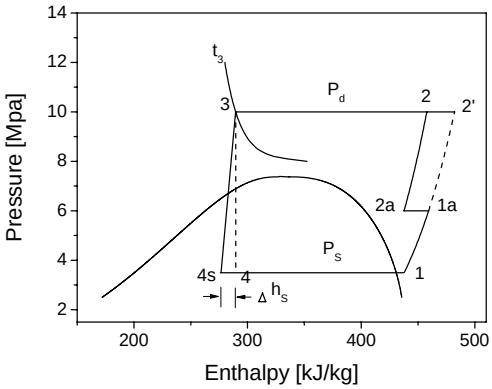

Fig. 2 P-h diagram of a CO_2 transcritical cycle with expander-compressor unit

Fig.1 shows a schematic diagram of a two-stage compression CO_2 cycle with an expander-compressor unit. Expansion valve is replaced by the expander which is directly coupled to the first-stage compressor via a common shaft. P-h diagram of this system is illustrated in Fig.2. Isentropic expansion along the line 3-4s is assumed to take place and the refrigerating effect is increased by Δh_s compared with that of isenthalpic process of the line 3-4. The first stage compressor driven by the expander output raises the gas pressure from P_s (P_1) to P_{1a} along the line 1-1a. Horizontal line 1a-2a indicates inter-stage cooling between the first and second stage compressors. In this study, 5°C was assumed for the inter-stage cooling.

A schematic of the scroll expander-compressor unit is illustrated in Fig.3. The CO2 coming out of the gas cooler enters into the expander inlet through the suction pipe(⑥), runs the orbiting scroll(②), while expanding in the expander chambers, and exits into the evaporator through the discharge pie(⑦). Torque produced by the orbiting scroll operation is transmitted to the compressor side via the crank shaft(⑤). The CO2 from the evaporator outlet enters into the compressor suction manifold through the suction pipe(⑩). Gas is compressed in the compression chambers formed between the fixed and orbiting scrolls(⑪,⑫), and discharged through the discharge pipe(⑰) into the second stage compressor, which is the main compressor for this case.

2.1 Expander side

Since expansion mode can be obtained by operating a scroll compressor in reverse, the discharge volume of a scroll compressor can be regarded as the suction volume for the corresponding scroll expander. The suction and discharge volumes of a scroll expander are given by the following equations, respectively.

$$V_{th,e} = 2\pi a h r_s(2\phi_{a,e} + \pi), \quad V_{4s} = 2\pi a h r_s(2\phi_{e,e} - \pi) \qquad \text{(1a), (1b)}$$

For the CO_2 trans-critical cycle with the expander-compressor unit as in Fig.2, the cooling capacity is related to the displacement volume of the scroll expander.

$$Q_e = \rho_3 \frac{V_{th,e}}{\eta_{v,e}} \frac{N}{60}(h_1 - h_4 + \Delta h_s) \qquad (2)$$

Discharge volume V_{4s} is obtained from the built-in volume ratio of the expander, $V.R$, which can be related to the CO_2 densities at the inlet and outlet of the expander.

$$V.R. = \frac{V_{4s}}{V_{th,e}} = \frac{\dot{m}/\rho_{4s}}{\dot{m}/\rho_3} = \rho_3\left(\frac{x_{4s}}{\rho_{g,4s}} + \frac{1 - x_{4s}}{\rho_{l,4s}}\right) \qquad (3)$$

Scroll wrap end angle of the expander $\phi_{e,e}$ is determined from V_{4s} by the equation (1b).

The volumetric, isentropic, mechanical, and total efficiencies of the expander are defined by the following equations, respectively.

$$\eta_{v,e} = \dot{m}_{th,e}/\dot{m}_r, \ \eta_{i,e} = \frac{L}{\dot{m}_r \Delta h_s}, \ \eta_{m,e} = L_s/L, \ \eta_e = \frac{L_s}{\dot{m}_r \Delta h_s} = \eta_{i,e}\eta_{m,e} \qquad \text{(4),(5),(6),(7)}$$

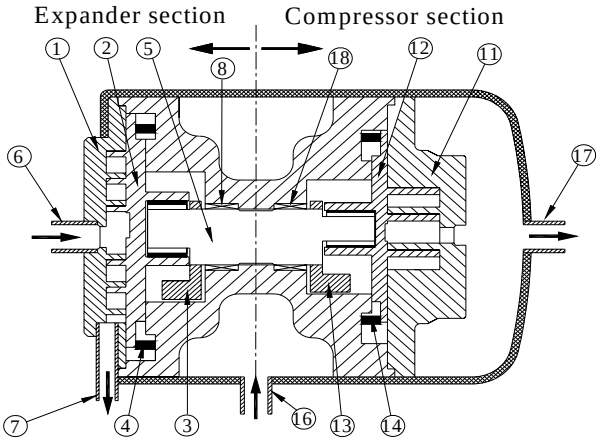

Expander		Compressor	
1	Fixed scroll	11	Fixed scroll
2	Orbiting scroll	12	Orbiting scroll
3	Balance weight	13	Balance weight
4	Oldham-ring	14	Oldham-ring
5	Crank shaft	15	Crank shaft
6	Suction pipe	16	Suction pipe
7	Discharge pipe	17	Discharge pipe
8	Journal bearing	18	Journal bearing

Fig. 3 Expander-compressor unit

Here, $\dot{m}_{th,e}$ is defined by $\rho_3 V_{th,e}(N/60)$, and L is the power produced by the CO_2 expansion in the expansion chambers.

2.2 Compressor side

Discharge pressure of the first stage compressor depends on the power output of the expander. The power required to raise the pressure from P_s to P_{1a} is given by the following equation.

$$L_{ad} = \eta_c L_s = \frac{n}{n-1} P_s \frac{\dot{m}_r}{\rho_s}\left[\left(\frac{P_{1a}}{P_s}\right)^{(n-1)/n} - 1\right] \tag{8}$$

In other words, the built-in pressure ratio of the first stage compressor, P_{1a}/P_s, is determined by the expander output. Since the mass flow rate of the compressor is the same as that of the expander, the displacement volume of the first stage compressor is given by the following equation.

$$V_{th,c} = \frac{\rho_3}{\rho_s}\frac{V_{th,e}}{\eta_{v,e}\eta_{v,c}} \tag{9}$$

Discharge volume of the first stage compressor V_{1a} is obtained from the built-in pressure ratio.

$$\frac{V_{th,c}}{V_{1a}} = \left(\frac{P_{1a}}{P_s}\right)^{1/n} \tag{10}$$

The displacement and discharge volumes of the scroll compressor are related to the scroll wrap configuration factors as before for the expander.

$$V_{th,c} = 2\pi a h r_s(2\phi_{e,c} - \pi), \quad V_{1s} = 2\pi a h r_s(2\phi_{a,c} + \pi) \tag{11a),(11b)}$$

The volumetric, isentropic, mechanical, and total efficiencies of the compressor are defined by the following equations, respectively.

$$\eta_{v,c} = \dot{m}_r / \dot{m}_{th,c},\ \eta_{i,c} = L_{ad}/L_i,\ \eta_{m,c} = L_i/L_s,\ \eta_c = \frac{L_{ad}}{L_s} = \eta_{i,c}\eta_{m,c} \tag{12),(13),(14),(15)}$$

2.3 Determination of the scroll configuration factors

Typical pressure and temperature conditions for heat pump water heater CO_2 cycles are shown in Table 1. For

Table 1 Operating conditions

Notation	Description	Value
t_1	Compressor suction temp.	4.2 [℃]
t_3	Gas cooler temp.	35 [℃]
P_s	Evaporator pressure	3.5 [MPa]
P_d	Gas cooler pressure	10 [MPa]
N	Compressor speed	3500 [rpm]

Table 2 Main specifications of scroll expander and compressor unit

Notation	Expander	Compressor
$P.R$	2.86(10/3.5)	1.21(4.24/3.5)
$V.R$	2.91	1.15
V_{th}	1.32 [cc]	12.05 [cc]
ϕ_a	239°	254°
ϕ_e	1229°	665°
t	4 [mm]	4 [mm]
h	4 [mm]	17.5 [mm]

design of the scroll expander and compressor, the following assumptions were initially made: $\eta_{v,e} = 85\%$, $\eta_{i,e} = 90\%$, $\eta_{m,e} = 90\%$ for the expander side, and $\eta_{v,c} = 97\%$, $\eta_{i,c} = 90\%$, $\eta_{m,c} = 90\%$ for the compressor side. For the main compressor the total compressor efficiency was assumed to be $\eta_{c,2} = 70\%$.

For the cooling capacity of 36,000 Btu/hr as a design requirement at the given operating conditions, the mass flow rate was 0.063kg/s with the initially assumed values of the efficiencies. The discharge pressure of the first stage compressor was estimated to be P_{1a} = 4.24 MPa. With these determined values together with the relations mentioned above, scroll configuration factors for the expander and compressor were determined as in Table 2.

3. NUMERICAL SIMULATION

3.1 Expander

For isentropic expansion, the pressure in an expander chamber can be obtained if the density $\boldsymbol{\rho_m}$ in the chamber is known.

$$\boldsymbol{P = P(\rho_m;\, s_3) \quad with \;\; s_3 = s_3(P_3;\, t_3)} \tag{16}$$

The density $\boldsymbol{\rho_m}$ in the expansion chamber is calculated as follows:

$$\boldsymbol{\rho_m = \frac{M(0) - \int_0^t \dot{m}_l dt}{V(t)}} \tag{17}$$

Here $\boldsymbol{\dot{m}_l}$ represents leakage through clearance between chambers, and it is given by

$$\boldsymbol{\dot{m}_l = c_v A_l P_{up} \sqrt{\frac{2n}{(n-1)RT_{up}}} \sqrt{\left(\frac{P_{dn}}{P_{up}}\right)^{2/n} - \left(\frac{P_{dn}}{P_{up}}\right)^{(k-1)/k}}} \tag{18}$$

Here subscripts $\boldsymbol{up}$ and $\boldsymbol{dn}$ denote upstream and downstream sides of the leakage clearance, respectively. Flow coefficient c_v was predetermined and data based over wide ranges of pressure and clearance by comparing the mass flow rate of ideal nozzle flow to that of Fanno flow. Gas forces are obtained from the gas pressure distribution in the expansion chambers.

Enthalpy $\boldsymbol{h}$ and the fraction of vapor $\boldsymbol{x}$ are obtained as functions of pressure only along a constant entropy line:

$$\boldsymbol{h = h(P;\, s_3)} \;,\; \boldsymbol{x = x(P;\, s_3)} \tag{19), (20}$$

As the CO_2 expands in the expander, the orbiting scroll is driven by the tangential component of the gas force produced in the expansion chambers. The tangential gas force $\boldsymbol{F_{tg}}$, torque $\boldsymbol{T}$ generated by the gas expansion, and the corresponding power $\boldsymbol{L}$ are written by the equations (21)-(23), respectively.

$$\boldsymbol{F_{tg} = \frac{1}{2\pi}\int P dV} \;,\; \boldsymbol{T = r_s F_{tg}} \;,\; \boldsymbol{L = \omega T} \tag{21),(22),(23}$$

Dynamics for the moving elements are to be solved to give friction losses at sliding surfaces. Eleven equations of force and moment balances on the orbiting scroll, Oldham-ring and sliding bush are set up with eleven unknowns: tangential and radial components of the orbiting scroll hub reaction, flank sealing force, four reactions at the Oldham-ring keys, reaction position from the thrust surface to the orbiting scroll base plate, and magnitude and arm of crank pin reaction(Kim *et al*, 1998). Journal bearing load at the crank shaft needs to be solved simultaneously with that of the compressor side. Boundary lubrication was assumed at the thrust surface, wrap flank and Oldham-ring keys, and hydrodynamic lubrication for the rest of the sliding surfaces. Friction coefficient was assumed 0.03 at the thrust surface, and 0.013 at the other boundary lubrications; for journal bearing, it was obtained as a function of Sommerfeld number and the bearing length to diameter ratio.
Shaft output is given by

$$L_s = L - (\Delta L_{thrust} + \Delta L_{flank} + \Delta L_{keys} + \Delta L_{CP} + \Delta L_{JB}) \tag{24}$$

3.2 Compressor

Pressure in a compression chamber is calculated by

$$P = P_s(\rho/\rho_s)^n, \quad \rho = M(t)/V \tag{25}$$

Leakage in the compression chamber was also taken into account for the mass calculation in the compression chamber. The rest of the modeling for the compressor section is similar to that of the expander.

4. RESULTS AND DISCUSSION

For the operating conditions shown in Table 1, computer simulation has been made on the performance of the expander-compressor unit. The scroll clearance was assumed to be 8 μm for both the wrap tip and the flank. Calculation results of the performance improvement for the CO_2 cycle due to the application of the expander-compressor unit were summarized in Table 3. While the system COP without the unit was 2.538, that of the system equipped with the unit was 3.134, resulting in the COP improvement of 23.5%. Increase in the refrigerating effect due to the isentropic expansion was 8.6% and reduction in the main compressor input due to the auxiliary compressor operation was 12.1%. Efficiencies of the expander and the coupled auxiliary compressor were listed in Table 4. Total efficiencies were 54.43% and 85.61% for the expander and the compressor, respectively. Mechanical efficiency of the expander was quite lower than that assumed at the design stage. It is mainly because of the large axial gas force developed in the expansion chambers.
Fig.4 shows the pressure change in the expansion chamber. The pressure decrease began to occur even before the end of the suction process due to leakage through scroll wrap clearance. Before crossing the saturation line the pressure decrease was very steep, and it became slow afterward. Fig.5 shows P-V diagram of the auxiliary compressor. Over-compression took place in the initial stage of the discharge process. The expander output was not large enough to build the discharge pressure designated at the design stage for the first stage compressor.
Fig.6 shows the influence of the suction pressure on the pressure changes of the expander and compressor: When P_s was lower than the design suction pressure for the expander, under-expansion was encountered near the end of the expansion process. Over-expansion occurred for higher P_s than the design suction pressure. For the compressor side,

Table 3 Improvement of CO_2 cycle performance at design condition : P_s =3.5MPa, P_d =10MPa, t_3 =35°C

	Without Expander	With Expander	Ratio
Expander Power Output	-	0. 696 [kW]	-
Cooling Capacity	9.35 [kW]	10.155kW]	1.086
Compressor Work (Main/Auxiliary)	(3.684 / -) [kW]	(3.24 / 0.696) [kW]	0.879
COP	2.538	3.134	1.235

Table 4 Expander-compressor efficiencies

Efficiency[%]	Expander		Compressor	
Volumetric	$\eta_{v,e}$	86.51	$\eta_{v,c}$	95.94
Isentropic	$\eta_{i,e}$	86.12	$\eta_{i,c}$	94.17
Mechanical	$\eta_{m,e}$	63.2	$\eta_{m,c}$	90.90
Total	η_e	54.43	η_c	85.61

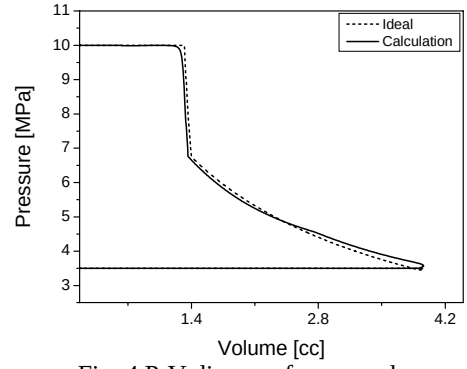

Fig. 4 P-V diagram for expander

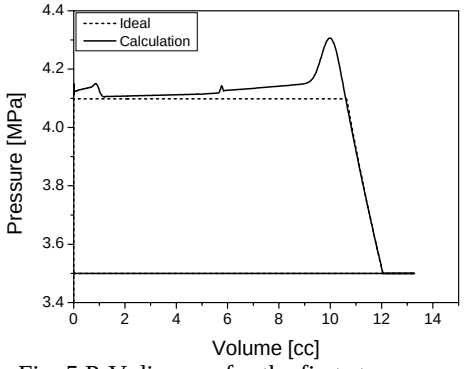

Fig. 5 P-V diagram for the first stage compressor

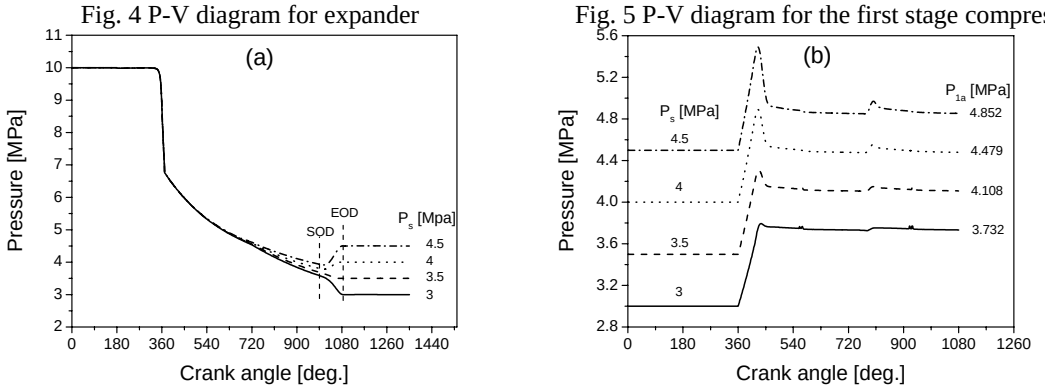

Fig. 6 P-θ diagram of expander-compressor unit at various suction pressures: (a) expander, (b) compressor

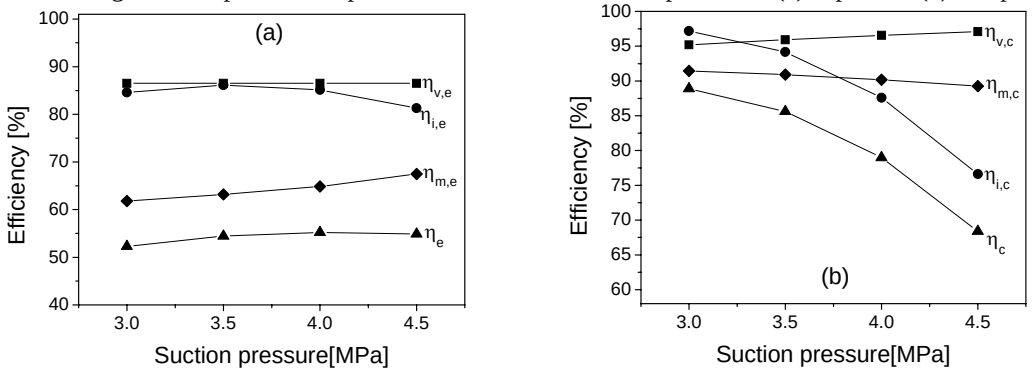

Fig. 7 Expander-compressor efficiencies at various suction pressures: (a) expander, (b) compressor

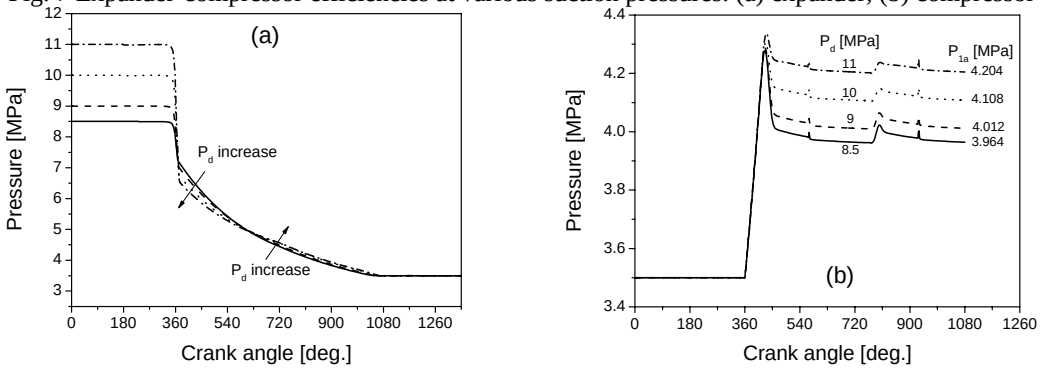

Fig. 8 P-θ diagram of expander-compressor unit at various discharge pressures: (a) expander, (b) compressor

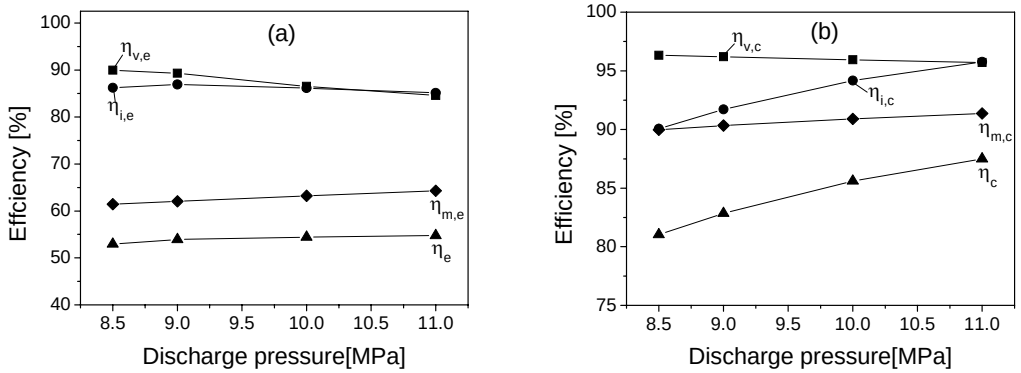

Fig. 9 Expander-compressor efficiencies at various discharge pressures: (a) expander, (b) compressor

over-compression became more severe as P_s became higher, but it was alleviated for lower P_s. Variation of the expander and compressor efficiencies with P_s are shown in Fig.7(a) and (b), respectively. Volumetric efficiency of the expander $\eta_{v,e}$ was more or less insensitive to changes of P_s, while that of the compressor $\eta_{v,c}$ increased with increasing P_s. Isentropic efficiency of the expander $\eta_{i,e}$ became a maximum at the design pressure, but that of the compressor $\eta_{i,c}$ decreased rapidly with increasing P_s, because the operating pressure ratio became smaller than the built-in pressure ratio. Mechanical efficiency of the expander $\eta_{m,e}$ increased with increasing P_s: It is due to decrement of the pressure force acting on the thrust surface. As a consequence, total efficiency showed a mild increment for the expander and a rather rapid drop for the compressor with increasing P_s.

Fig.8 shows the influence of P_d on the pressure changes of the expander and compressor: As P_d increased, the pressure decrease became slower in the two-phase region. For the compressor, more power input was transmitted from the expander with increasing P_d, resulting in reducing over-compression loss. Effects of changing P_d on the expander and compressor efficiencies are shown in Fig.9(a) and (b), respectively. For both the expander and compressor, volumetric efficiency decreased with increasing P_d. Isentropic efficiency of the compressor $\eta_{i,c}$ increased with increasing P_d, since the operating pressure ratio approached closer to the built-in pressure ratio with increasing P_d. Mechanical efficiency $\eta_{m,e}$ also increased with increasing P_d: It is because increasing rate of the expansion power by running orbiting scroll was larger than that of the mechanical loss as P_d increased. All these yielded to increasing total efficiencies of the expander and compressor, although η_e of the expander increased very slowly.

Fig.10 shows the effects of the suction pressure, discharge pressure, and the inlet temperature of the expander on the relative COP improvement of the cycle by using the expander-compressor unit. COP_{ratio} in the ordinate indicates the ratio of COP of the system with the expander-compressor unit to that of the system without the unit. As P_s increased from 3.0MPa to 4.5MPa, the relative COP improvement decreased from 27.5% to 17.4%. The effect of P_d on the relative COP improvement was not large. Also the inlet temperature of the expander t_3 had quite an influence on the relative COP improvement: It increased from 20.7% to 24.3% as t_3 increased from 20°C to 40 °C.

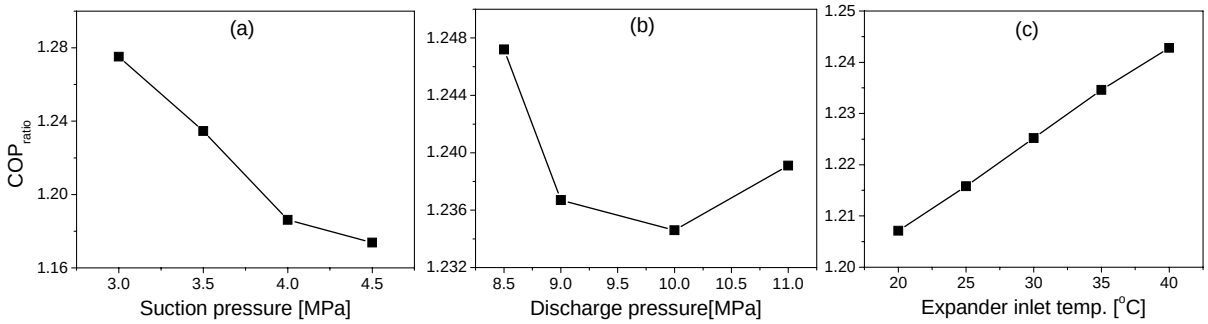

Fig. 10 COP improvement by using expander-compressor unit: (a) $P_d = 10MPa,\ t_3 = 35^oC$
(b) $P_s = 3.5MPa,\ t_3 = 35^oC$ (c) $P_d = 10MPa,\ P_s = 3.5MPa$

5. CONCLUSIONS

In an analytical study on the COP improvement of a two-stage compression CO_2 trans-critical cycle by the application of a combined scroll expander-compressor unit,

- Conceptual design of the combined scroll expander-scroll compressor unit has been made.
- Performance analysis has been carried when the compressor of the unit was used as the first stage compressor.
- At the design operating condition, the total efficiency of the expander was calculated to be 54.4%, and that of the compressor was 85.6% with the scroll wrap clearance of 8 μm. COP improvement by the use of this unit was 23.5%.
- Expander efficiency could be increased by reducing expansion chamber area, which could be done with increasing wrap height.
- The compressor efficiency decreased rapidly when the operating pressure ratio became far from the built-in pressure, whereas the expander efficiency was rather insensitive to pressure changes.
- Relative COP improvement decreased from 27.5% to 17.4% as the suction pressure increased from 3Mpa to 4.5Mpa, while the effect of the discharge pressure changes was not large. Also the inlet temperature of the expander had quite an influence on the relative COP improvement.

NOMENCLATURE

a	base circle radius	(m)	**Subscripts**	
F_{tg}	tangential gas force	(N)	*ad*	adiabatic
h	wrap height	(m)	*c*	compressor
L	power	(W)	*e*	expander
$\dot{m}$	mass flowrate	(kg/s)	*g*	gas
n	polytropic index	(-)	*i*	isentropic
N	compressor speed	(rpm)	*l*	liquid
P_s	suction pressure	(Pa)	*m*	mechanical, mixture
Q_e	cooling capacity	(Btu/hr)	*r*	real
r_s	orbiting radius	(m)	*s*	shaft, suction
s	entropy	(kJ/kg K)	*v*	volumetric
T	Temperature	(^oC)	*1,1a,2,3,4,4s*	points in Fig. 2
V	volume	(m^3)		
x	vapor quality	(-)		
η	efficiency	(%)		
ϕ_a	cutter angle	(degree)		
ϕ_e	involute end angle	(degree)		
ρ	density	(kg/m^3)		

REFERENCES

Nickl, J., Will, G., Kraus, W.E., and Quack, H., 2003, Third generation CO_2 expander, *International Congress of Refrigeration*, Washington, D.C., Paper No. ICR0571

Zha S., Ma, Y., and Sun X., 2003, The development of CO_2 expander in CO_2 transcritical cycles, *International Congress of Refrigeration*, Washington D.C., Paper No. ICR0089

Fukuta, M, Yanagisawa, T., and Radermacher, R., 2003, Performance prediction of vane type expander for CO_2 cycle,' *International Congress of Refrigeration*, Washington D.C., Paper no ICR0251

Preissner M., 2001, Carbon dioxide vapor compression cycle improvement with focus on scroll expander, Ph.D dissertation, University of Maryland, USA

Westphalen, D. and Dieckmann, J., 2004, Scroll expander for carbon dioxide air conditioning cycles, *International Refrigeration and Air Conditioning Conference*, Purdue, USA, Paper No R023.

H.J.Kim, J.K.Lee, D.K.Shin, 1998, "Design of Phase Angled Balance Weights for an Inverter Driven Scroll Compressor," *Proceedings of International Compressor Engineering Conference*, pp.749-754.